A RESOLUTION PRESERVING TEXTURAL TRANSFORM FOR IMAGES

R. M. Haralick

Remote Sensing Laboratory and Department of Electrical Engineering
University of Kansas
Lawrence, Kansas 66045

Abstract

This paper describes an image dependent two-dimensional non-linear spatial filter designed to be a resolution preserving textural feature extractor for image data. The textural transform is based on the neighboring grey tone co-occurrence properties of the image to be transformed. Classification experiments with the textural transform on satellite multispectral scanner imagery over forrested areas show that higher identification accuracy can be achieved when using combined spectral and textural information than when using only spectral information.

Introduction: What is Texture?

Spatial environments can be understood as being spatial distributions of various area-extensive objects having characteristic size and reflectance or emissive qualities. The spatial organization and relationships of the area-extensive objects appear as spatial distributions of grey tone on imagery taken of the environment. We call the pattern of spatial distributions of grey tone, texture.

Figure 1, taken from Lewis (1971), illustrates how texture relates to geomorphology. There are some plains, low hills, high hills, and mountains in the Panama and Columbia area taken by the Westinghouse AN/APQ97 K-band radar imager system. The plains have apparent relief of 0-50 meters, the hills have apparent relief of 50-350 meters, and the mountains have apparent relief of more than 350 meters. The low hills have little dissection and are generally smooth convex surfaces whereas the high hills are highly dissected and have prominent ridge crests.

The mountain texture is distinguishable from the hill texture on the basis of the extent of radar shadowing (black tonal areas). The mountains have shadowing over more than half the area and the hills have shadowing over less than half the area. The hills can be subdivided from low to high on the basis of the abruptness of tonal change from terrain front slope to terrain back slope.

Figure 2, taken from MacDonald (1970), illustrates how texture relates to geology. There are some igneous and sedimentary rocks in Panama taken by the Westinghouse AN/APQ97 K-band radar imagery system. Figure 2 i, k, l show a fine textured drainage pattern which is indicative of non-resistant fine-grained sedimentary rocks. The coarser texture with rugged and peaked divides (Figure 2a, b, c, d, e,)is indicative of igneous rocks. When erosion has nearly base-leveled an area, the texture takes on a hummocky appearance of Figure 2c.

Figure 3, taken from Haralick and Anderson (1971), illustrates how texture relates to land use categories. Here, there are six land use categories as they appear on panchromatic aerial photography. Notice how the texture of the wooded area is coarser and more definite than the scrub area. The swamps and marsh generate finer textures than those generated from wood or scrub areas. The swamp texture is finer than and shows more gradual grey tone change than the marsh generated textures.

Figure 4 is taken in the Pisgah Crater area and shows some examples where the same type of terrain generates a variety of textures within the same texture family. Here, the texture changes are due to the way the vegetation increases in size and disperses.

Techniques of Quantifying Texture

There have been six basic approaches to the measurement and quantification of image texture: autocorrelation functions (Kaizer, 1955), optical transforms, (Lendaris and Stanley, 1970), digital transforms, (Gramenopoulos, 1973; Hornung and Smith, 1973; Kirvida and Johnson, 1973), edgeness (Rosenfled and Thurston, 1971), structural elements, (Matheron, 1967; Serra, 1973), and spatial grey tone co-occurrence probabilities, (Haralick et al., 1973). The first three of these approaches are related in that they all measure spatial frequency directly or indirectly. Spatial frequency is related to texture because fine textures are rich in high spatial frequencies while coarse textures are rich in low spatial frequencies.

An alternative to viewing texture as spatial frequency distribution is to view texture as amount of edge per unit area. Coarse textures have a small number of edges per unit area. Fine textures have a high number of edges per unit area.

The structural element approach uses a matching procedure to detect the spatial regularity of shapes called structural elements in a binary image. When the structural elements themselves are single resolution cells, the information provided by this approach is the autocorrelation function of the binary image. By using larger and more complex shapes, a more generalized autocorrelation can be computed.

The grey tone co-occurrence approach characterizes texture by the spatial distribution of its grey tones. Coarse textures are those for which the distribution changes only slightly with distance and fine textures are those for which the distribution changes rapidly with distance.

Optical Processing Methods and Texture

Edward O'Neill's (1956) article on spatial filtering introduced the engineering community to the fact that optical systems can perform filtering of the kind used in communication systems. In the case of the optical systems, however, the filtering is two-dimensional. The basis for the filtering capability of optical systems lies in the fact that the light amplitude distributions at the front and back focal planes of lens are Fourier Transforms of one another. The light distribution produced by the lens is more commonly known as the Fraunhofer diffraction pattern. Thus, optical methods facilitate two-dimensional frequency analysis of images.

The paper by Cutrona et al. (1960) provides a good review of optical processing methods for the interested reader. More recent books by Goodman (1968), Preston (1972), Shulman (1970) comprehensively survey the area.

In this section, we describe the experiments done by Lendaris and Stanley, Egbert et al., and Swanlund using optical processing methods in aerial or satellite imagery. Lendaris and Stanley (1970) illuminated small circular sections of low altitude aerial photography and used the Fraunhofer diffraction pattern as features for identifying the sections. The circular sections represented a circular area on the ground of 750 feet. The major category distinction they were interested in making was man-made versus non man-made. They further subdivided the man-made category into roads, road intersections, buildings, and orchards.

The pattern vectors they used from the diffraction pattern consisted of 40 components. Twenty components were averages of the energy in 9^{o} wedges of the diffraction pattern. They obtained over 90 per cent identification accuracy.

Egbert et al. used an optical processing system to examine the texture of ERTS imagery over Kansas. They used circular areas corresponding to a ground diameter of about 23

miles and looked at the diffraction patterns for the areas when they were snow covered and when they were not snow covered. They used a diffraction pattern sampling unit have 32 sector wedges and 32 annular rings to sample and measure the diffraction patterns. (See Jensen (1973) for a description of the sampling unit and its use in coarse diffraction pattern analysis). They were able to interpret the resulting angular orientation graphs in terms of dominant drainage patterns and roads but were not able to interpret the spatial frequency graphs which all seem to have had the same character: the higher the spatial frequency, the less the energy in that frequency band.

Swanlund (1969) has done work using optical processing on aerial images to identify species of trees. Using imagery obtained from Itasca State Park in northern Minnesota, photo-interpreters identified five (mixture) species of trees on the basis of the texture: Upland Hardwoods, Jack pine overstory/Aspen understory/Upland Hardwoods understory, Red pine overstory/Aspen understory, and Aspen. They achieved classification accuracy of over 90 percent.

Texture and Edges

The autocorrelation function, the optical transforms, and the fast digital transforms (FFT and FHT) basically all reference texture to spatial frequency. Rosenfeld and Thurston (1971) conceive of texture not in terms of spatial frequency but in terms of edgeness per unit area. An edge passing through a resolution cell is detected by comparing the values for local properties obtained in pairs of nonoverlapping neighborhoods boarding the resolution cell. To detect microedges, small neighborhoods must be used. To detect macroedges, large neighborhoods must be used.

The local property which Rosenfeld and Thurston suggested was the quick Roberts gradient (the sum of the absolute value of the differences between diagonally opposite neighboring pixels). Thus, a measure of texture for any subimage is obtained by computing the Roberts gradient image for the subimage and from it determining the average value of the gradient in the subimage. Triendle (1972) uses the Laplacian instead of the Roberts gradient.

Sutton and Hall (1972) extended Rosenfeld and Thurstons idea by making the gradient a function of the distance between the pixels. Thus, for every distance d and subimage I defined over a neighborhood N of resolution cells, they compute

$$g(d) = \sum_{(i,j)\in N} \{|I(i,j) - I(i+d,j)| + |I(i,j) - I(i-d,j)| + |I(i,j) - I(i,j+d)| + |I(i,j) - I(i,j-d)|\}.$$

The graph of g(d) is like the graph of the minus autocorrelation function translated vertically.

Sutton and Hall applied this textural measure in a pulmonary disease identification experiment using radiographic imagery and obtained identification accuracy in the 80 percentile range for discriminating between normal and abnormal lungs when using a 128 x 128 subimage.

Digital Transform Methods and Texture

In the digital transform method of texture analysis, the digital image is typically divided into a set of non-overlapping small square subimages. Suppose the size of the subimage is n x n resolution cells, then the n^2 grey tones in the subimage can be thought of as the n^2 components of an n^2-dimensional vectors. In the transform technique, each of these vectors is re-expressed in a new coordinate system. The Fourier Transform uses the sine-cosine basis set. The Hadamard Transform uses the Walsh function basis set, etc. The point to the transformation is that the basis vectors of the new coordinate system have an interpretation that relates to spatial frequency (sequency) and since frequency (sequency) is a close relative of texture, we see that such transformation can be useful.

Gramenopoulos (1973) used a transform technique using the sine-cosine basis vectors (and implemented it with the FFT algorithm) on ERTS imagery to investigate the power of texture and spatial pattern to do terrain type recognition. He used subimages of 32 by 32 resolution cells and found that on Phoenix, Arizona ERTS image 1049-17324-5 spatial frequencies larger than 3.5 cycles/km and smaller than 5.9 cycles/km contain most of the information needed to discriminate between terrain types. The terrain classes were: clouds, water, desert, farms, mountains, urban, riverbed, and cloud shadows. He achieved an overall identification accuracy of 87 percent.

Hornung and Smith (1973) have done work similar to Gramenopoulos but with aerial multispectral scanner imagery instead of ERTS imager. Maurer (1974) used Fourier series analysis on some color aerial film to obtain textural features to help determine crop types.

Kirvida and Johnson (1973) compared the fast Fourier, Hadamard, and Slant Transforms for textural features on ERTS imagery over Minnesota. They used 8 x 8 subimages and five categories: Hardwoods, Conifers, Open, Water, City. Using only spectral information, they obtained 74 percent correct identification accuracy. When they added textural information, they increased they identification accuracy to 99 percent. They found little difference between the different transform methods.

Spatial Grey Tone Dependence: Co-occurance

One aspect of texture is concerned with the spatial distribution and spatial dependence among the grey tones in a local area. Darling (1968) used statistics obtained from the nearest neighbor grey tone transition matrix to measure this dependence for satellite images of clouds and was able to identify cloud types on the basis of their texture. Read and Jayaramamurthy (1972) divided an image into all possible (overlapping) subimages of reasonably small and fixed size and counted the frequency for all the distinct grey tone patterns. This is one step more general than Darling but one that requires too much memory if the grey tones can take on very many values. Haralick (1971) and Haralick et al. (1972, 1973) suggested an approach which is a compromise between the two. He measures the spatial dependence of grey tones in a co-occurrence matrix for each fixed distance and/or angular spatial relationship and uses statistics of the matrix as measures of image texture.

The co-occurrence matrix $P = (p_{ij})$ has its $(i,j)^{th}$ entry p_{ij} defined as the number of times grey tone i and grey tone j occur in resolution cells of a subimage have a specified spatial relation, such as distance 1 neighbors. The textural features for the subimage are obtainable from the co-occurrence matrix by measures such as

$$\sum_i \sum_j p_{ij}^2 , \quad \sum_i \sum_j p_{ij} \log p_{ij} ,$$

and

$$\sum_i \sum_j \frac{p_{ij}}{1 + |i-j|} .$$

Haralick et al. (1973) list 14 different kinds of measures.

Using statistics of the co-occurrence matrix, Haralick performed a number of identification experiments. On a set of aerial imagery and eight terrain classes (old residential, new residential, lake, swamp, marsh, urban, railroad yard, scrub or wooded), he obtained 82 percent corrent identification with 64 x 64 subimages. On an ERTS Monterey Bay, California image, he obtained 84 percent correct identification using 64 x 64 subimages and both spectral and textural features on seven terrain classes: coastal forest, woodlands, annual grasslands, urban areas, large irrigated fields, small irrigated fields, and water. On a set of sandstone photomicrographs, he obtained 89 percent correct identification on five sandstone classes: Dexter-L, Dexter-H, St. Peter, Upper Muddy, Gaskel.

The wide class of images on which they found that grey tone co-occurrence carries much of the texture information is probably indicative of the power and generality of this approach.

A Textural Transform

Each of the approaches described for the quantification of textural features had the common property that the textural features were computed for subimages of typical sizes such as 8 x 8, 16 x 16, 32 x 32, or 64 x 64 resolution cells. To determine the textural features for one pixel we would naturally center a subimage on the specified resolution cell and compute the textural features for the subimage. If we had to determine the textural features for each pixel in an image we would be in for a lot of computation work and would significantly increase the size of our data set. Thus, the usual approach has been to divide the image into mutually exclusive subimages and compute the textural features on the selected subimages. Unfortunately, this procedure produces textural features at a coarser resolution than the original image.

In this section we generalize the grey tone co-occurrence textural feature extractor to the textural transform mode and show how by only doubling or tripling the computation time required to determine the grey tone co-occurrence matrix it is possible to produce a resolution preserving textural transform in which each pixel in the tranformed image has textural information about its own neighborhood derived from both local and global grey tone co-occurrence in the image. This kind of textural transform is in the class of image dependent non-linear spatial filters.

Let $Z_r \times Z_c$ be the set of resolution cells of an image I (by row-colum coordinates). Let G be the set of grey tones possible to appear on image I. Then I: $Z_r \times Z_c \to G$. Let R be a binary relation on $Z_r \times Z_c$ pairing together all those resolution cells in the desired spatial relation. The co-occurrence matrix P, P: $G \times G \to [0,1]$, for image I and binary relation R is defined by

$$P(i,j) = \frac{\#\{((a,b),(c,d)) \in R \mid I(a,b) = i \text{ and } I(c,d) = j\}}{\#R}$$

The textural transform J, J: $Z_r \times Z_c \to (-\infty, \infty)$, of image I relative to function f, is defined by

$$J(y,x) = \frac{1}{\#R(y,x)} \sum_{(a,b) \in R(y,x)} f[P(I(y,x), I(a,b))]$$

Assuming f to be the identity function, the meaning of J(y,x) is as follows. The set R(y,x) is the set of all those resolution cells in $Z_r \times Z_c$ in the desired spatial relation to resolution cell (y,x). For any resolution cell $(a,b) \in R(y,x)$, P (I(y,x), I(a,b)) is the relative frequency by which the grey tone I(y,x), appearing at resolution cell (y,x), and the grey tone I(a,b), appearing at resolution cell (a,b), co-occur together in the desired spatial relation on the entire image. The sum

$$\sum_{(a,b) \in R(y,x)} P(I(y,x), I(a,b))$$

is just the sum of the relative frequences of grey tone co-occurrence over all resolution cells in the specified relation to resolution cell (y,x). The factor $\frac{1}{\#R(y,x)}$, the reciprocal of the number of resolution cells in the desired spatial relation to (y,x) is just a normalizing factor.

Figure 5 illustrates a series of areas of an ERTS image taken over Michigan. These 100 x 100 images were transformed using the textural transform for spatial relation R consisting of all pairs of resolution cells which are 8-neighboring. These are shown in Figure 6. Grey tones which are white are indicative of frequently occurring textural patterns in the corresponding spatial locations on the original subimage. Grey tones which are black are indicative of infrequently occurring textural patterns in the corresponding spatial locations on the original subimage.

To test the discrimination ability of the textural transform, we selected six land use categories in the forested Leeds region in South Dakota:

(1)	P-W	Wet pasture
(2)	P-D	Dry pasture
(3)	C2-SH	Type 2 conifer in shade
(4)	C2-SU	Type 2 conifer in sunshine
(5)	C1-SU	Type 1 conifer in sunshine
(6)	TR	Transition region

Figure 7 shows a contingency table of identification results on a SKYLAB image taken over the Leeds region. Spectral bands 0.68-0.76 and 0.98-1.08 μm were used. When the textural transform of band 0.68-0.76 μm was added as an additional feature, the results of the contingency table in Figure 8 were obtained. This is an improvement of 11%.

References

Cutrona, L. J., E. N. Leith, C.J. Palermo, and L. J. Porcello, "Optical Data Processing and Filtering Systems," IRE Transactions on Information Theory, Vol. , No. , June, 1960, pp. 386-400.

Goodman, J. W., Introduction to Fourier Optics, McGraw-Hill, New York, 1968.

Gramenopoulos, N., "Terrain Type Recognition Using ERTS-1 MSS Images," Symposium on Significant Results Obtained from the Earth Resources Technology Satellite, NASA SP-327, March, 1973, pp. 1229-1241.

Haralick, R. M., "A Texture-Context Feature Extraction Algorithm for Remotely Sensed Imagery," Proceedings 1971 IEEE Decision and Control Conference, Gainesville, Florida, December 15-17, 1971, pp. 650-657.

Haralick, R. M., K. Shanmugam, and I. Dinstein, "On Some Quickly Computable Features for Texture," Proceedings of the 1972 Symposium on Computer Image Processing and Recognition, University of Missouri, Vol. 2, August, 1972, pp. 12-2-1 to 12-2-10.

Haralick, R. M., K. Shanmugam, and I. Dinstein, "Textural Features for Image Classification," IEEE Transactions on Systems, Man, and Cybernetics, Vol. SMC-3, No. 6, November, 1973, pp. 610-621.

Hornung, R. J. and J. A. Smith, "Application of Fourier Analysis to Multispectral/Spatial Recognition," Management and Utilization of Remote Sensing Data ASP Symposium, Sioux Falls, South Dakota, October, 1973.

Jensen, N., "High-Speed Image Analysis Techniques," Photogrammetric Engineering, Vol. XXXIX, No. 12, December, 1973, pp. 1321-1328.

Kaizer, H., "A Quantification of Textures on Aerial Photographs," Boston University Research Laboratories, Technical Note 121, 1955, AD 69484.

Kirvida, L. and G. Johnson, "Automatic Interpretation of Earth Resources Technology Satellite Data for Forest Management," Symposium on Significant Results Obtained from the Earth Resources Technology Satellite, NASA SP-327, March, 1973, pp. 1076-1082.

Lendaris, G. G. and G. L. Stanley, "Diffraction-Pattern Sampling for Automatic Pattern Recognition," Proceedings of the IEEE, Vol. 58, No. 2, February, 1970, pp. 198-216.

Lewis, A. J., "Geomorphic Evaluation of Radar Imagery of Southeastern Panama and Northwestern Columbia," CRES Technical Report No. 133-18, University of Kansas Center for Research, Inc., Lawrence, Kansas, February, 1971.

MacDonald, H. C., "Geologic Evaluation of Radar Imagery from Darien Province, Panama," CRES Technical Report No. 133-6, University of Kansas Center for Research, Inc., Lawrence, Kansas, 1970.

Matheron, G., Elements Pour Une Theorie des Milieux Poreux, Masson, Paris, 1967.

Maurer, H., "Texture Analysis with Fourier Series," Proceedings of the Ninth International Symposium on Remote Sensing of Environment, Environmental Research Institute of Michigan, Ann Arbor, Michigan, April, 1974, pp. 1411-1420.

O'Neill, E., "Spatial Filtering in Optics," IRE Transactions on Information Theory, June, 1956, pp. 56-65.

Preston, K., Coherent Optical Computers, McGraw-Hill, New York, 1972.

Read, J. S. and S. N. Jayaramamurthy, "Automatic Generation of Texture Feature Detectors," IEEE Transactions on Computers, Vol. C-21, No. 7, July, 1972, pp. 803-812.

Rosenfeld, A. and M. Thurston, "Edge and Curve Detection for Visual Scene Analysis," IEEE Transactions on Computers, Vol. C-20, No. 5, May, 1971, pp. 562-569.

Serra, J. and G. Verchery, "Mathematical Morphology Applied to Fibre Composite Materials," Film Science and Technology, Vol. 6, 1973, pp. 141-158.

Shulman, A. R., Optical Data Processing, John Wiley & Sons, Inc., New York, 1970.

Sutton, R. and E. Hall, "Texture Measures for Automatic Classification of Pulmonary Disease," IEEE Transactions on Computers, Vol. C-21, No. 7, July, 1972, pp. 667-676.

Swanlund, G., "Honeywell's Automatic Tree Species Classifier," Honeywell Systems and Research Division, Report 9D-G-24, December 31, 1969.

Triendle, E. E., "Automatic Terrain Mapping by Texture Recognition," Proceedings of the Eighth International Symposium on Remote Sensing of Environment, Environmental Research Institute of Michigan, Ann Arbor, Michigan, October, 1972, pp. 771-776.

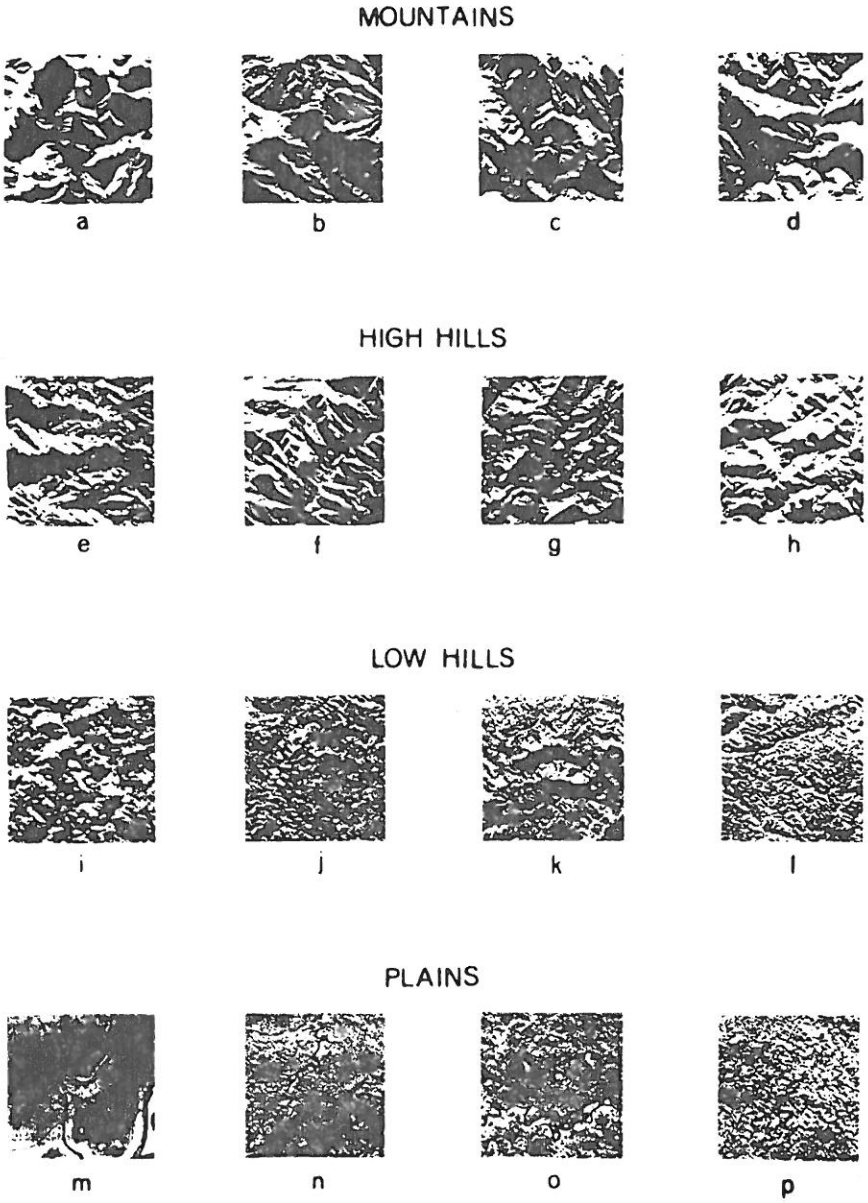

Figure 1 illustrates the texture generated by plains, hills, and mountains on K-band radar imagery, (taken from Lewis, 1971).

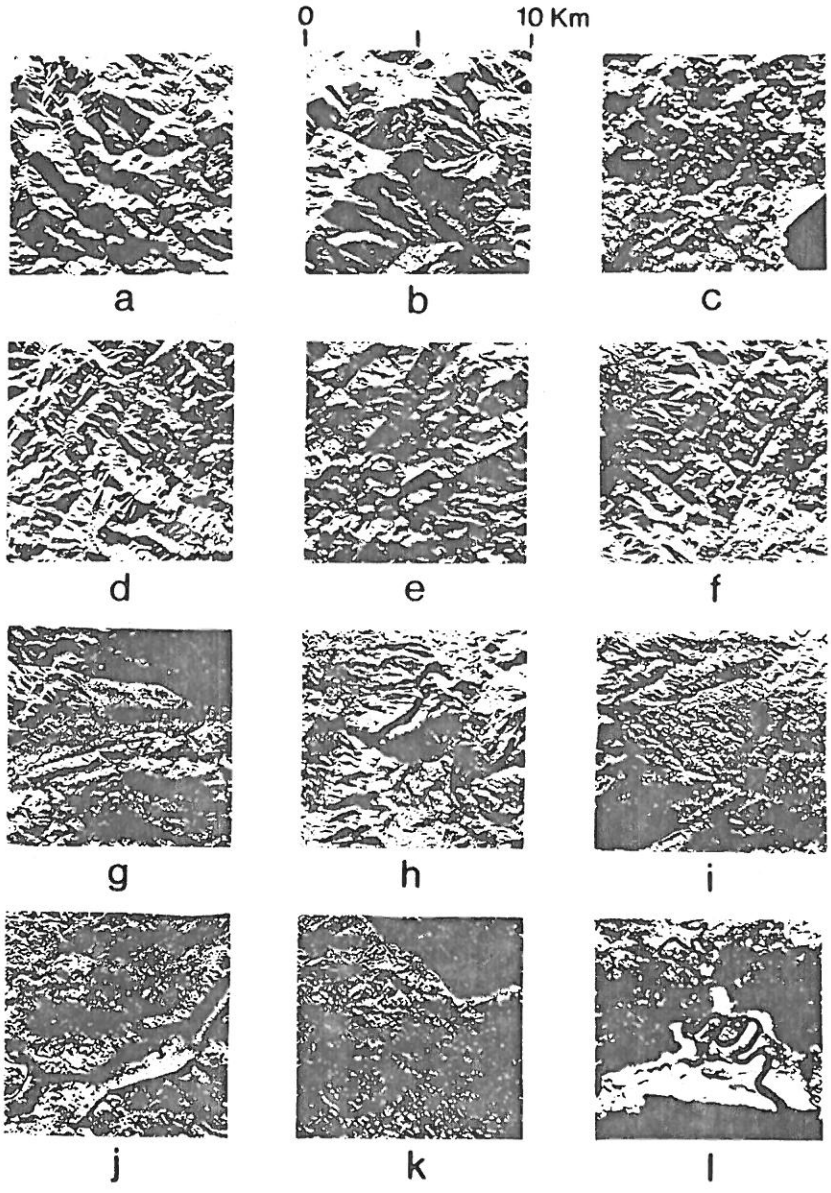

Figure 2 illustrates the texture generated by igneous and sediment rocks on K-band radar imagery, (taken from MacDonald, 1970).

MORE NATURAL-ENVIRONMENTAL TYPES OF SCENES

No. 1, SCRUB

(ETL NO. 815 - N2)

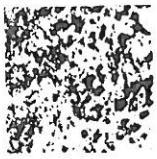

No. 66, MARSH

(ETL NO. 43 - T3B)

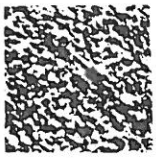

No. 41, SWAMP

(ETL NO. 43 - TB)

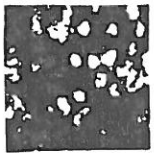

No. 56, MARSH

(ETL NO. 53 - T3A)

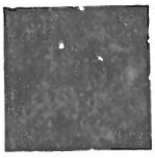

No. 7, HEAVILY WOODED AREA

(ETL NO. 697 - N1A)

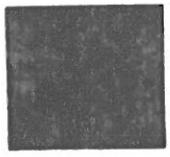

No. 27, RIVER

(ETL NO. 88 - R)

Figure 3 illustrates how environmental clutter relates to land-use categories, (taken from Haralick and Anderson, 1971).

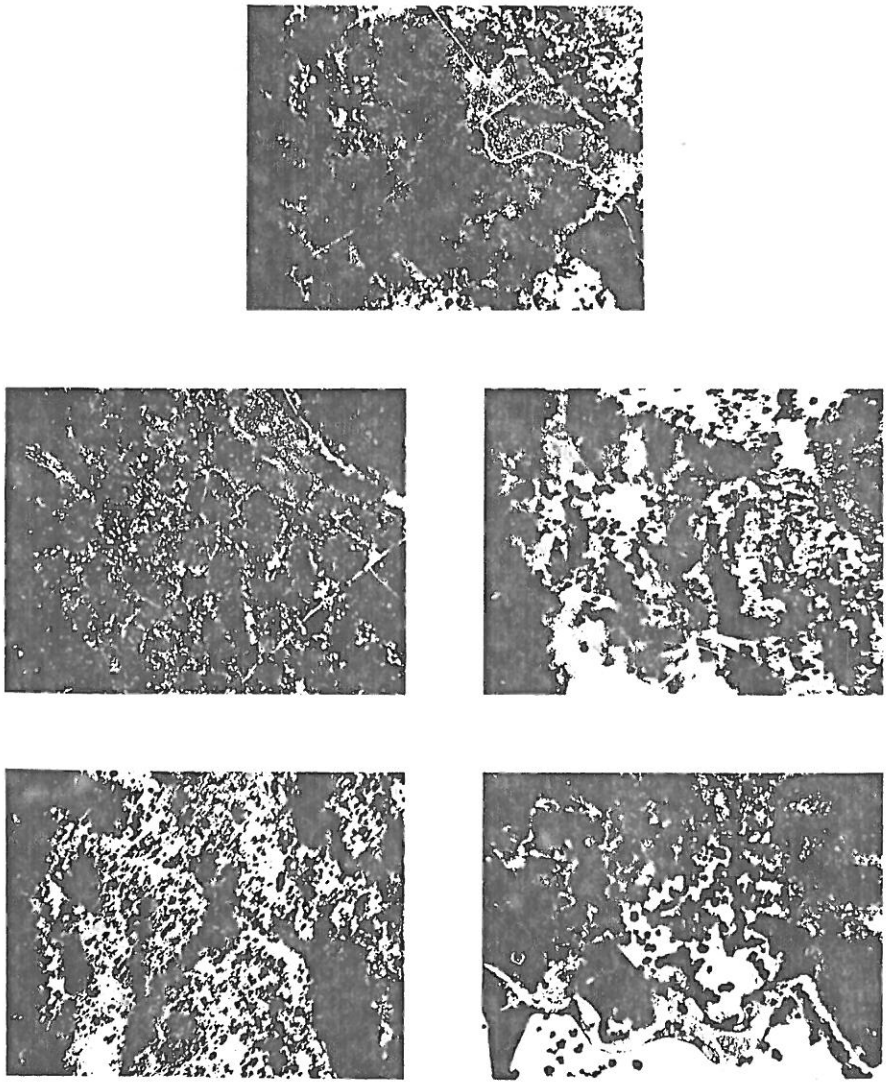

Figure 4 illustrates how the size and spacing of vegetation can cause texture to change from a fine texture to a coarse texture.

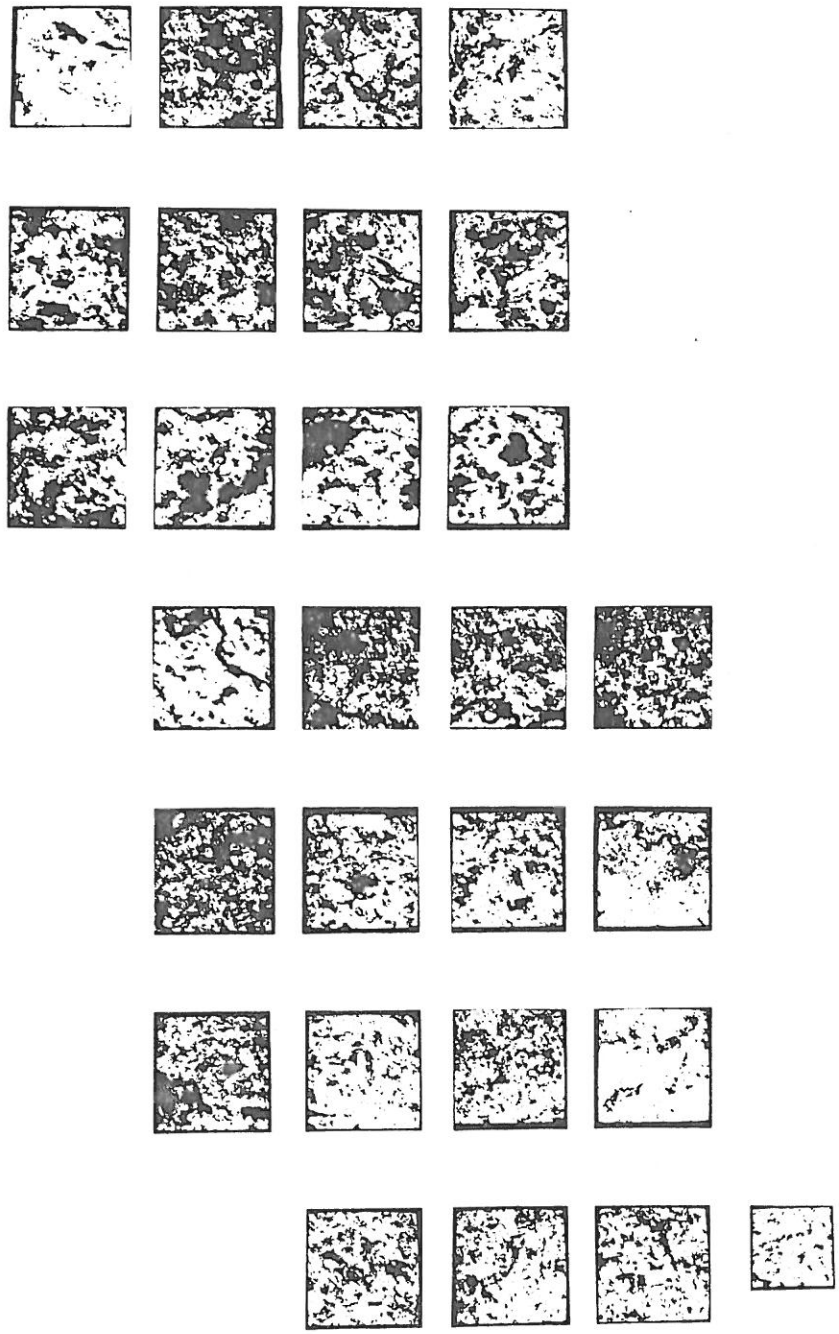

Figure 5 illustrates a series of areas of an ERTS image taken over Michigan.

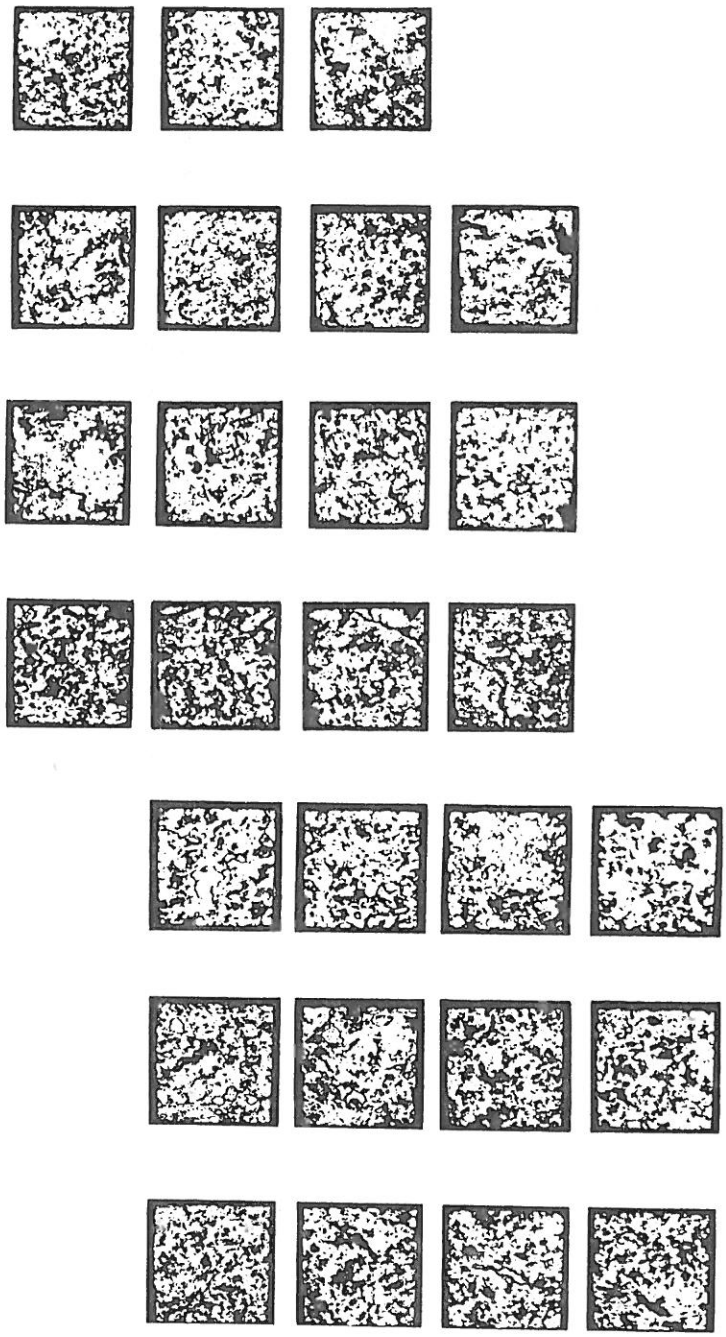

Figure 6 illustrates a series of 100 x 100 images that were transformed using the textural transform for spatial relation R consisting of all pairs of resolution cells which are 8-neighboring.

COL. = ASSIGN CAT ROW = TRUE CAT

	R DEC	P-W	P-D	C2-SH	C2-SU	C1-SU	TR	TOTAL	ERR	%ERR	%SD
UNKWN	4727	474	1160	2238	10976	6895	659	27129	0	0	0
P-W	19	47	8	0	0	0	0	74	8	15	3
P-D	22	12	114	0	0	0	0	148	12	10	2
C2-SH	21	0	0	92	11	5	0	129	16	15	2
C2-SU	30	1	2	4	238	16	0	291	23	9	1
C1-SU	46	6	3	3	25	229	11	323	48	17	1
TR	5	0	0	0	0	0	31	36	0	0	0
TOTAL	4870	540	1287	2337	11250	7145	701	28130	107	11	0
ERR	0	19	13	7	36	21	11	107			
% ERR	0	29	10	7	13	8	26	15			

Figure 8 shows the contingency table of identification results on the SKYLAB image of Figure 7 using the same spectral bands plus the textural transform of band 0.68-0.76 μm.

COL. = ASSIGN CAT ROW = TRUE CAT

	R DEC	P-W	P-D	C2-SH	C2-SU	C1-SU	TR	TOTAL	ERR	%ERR	%SD
UNKWN	0	232	1219	4010	11238	8806	1624	27129	0	0	0
P-W	0	36	12	0	0	0	26	74	38	51	5
P-D	0	6	116	1	1	0	24	148	32	22	3
C2-SH	0	0	0	105	17	7	0	129	24	19	3
C2-SU	0	0	16	9	241	23	2	291	50	17	2
C1-SU	0	3	2	7	25	261	25	323	62	19	2
TR	0	0	1	0	0	1	34	36	2	6	3
TOTAL	0	277	1366	4132	11522	9098	1735	28130	208	22	0
ERR	0	9	31	17	43	31	77	208			
% ERR	0	20	21	14	15	11	69	25			

Figure 7 shows the contingency table of identification results on a SKYLAB image taken over the Leeds region. The spectral bands were 0.68-0.76 and 0.98-1.08 μm.